Creation of arbitrary Dicke and NOON states of trapped-ion qubits by global addressing with composite pulses

Creation of arbitrary Dicke and NOON states of trapped-ion qubits by global addressing with composite pulses

Svetoslav S Ivanov[1,2,3]**, Nikolay V Vitanov**[2]
and Natalia V Korolkova[1]

[1] School of Physics and Astronomy, University of Saint Andrews, North Haugh, Saint Andrews, Fife KY16 9SS, UK
[2] Department of Physics, Sofia University, James Bourchier 5 Boulevard, 1164 Sofia, Bulgaria
E-mail: sivanov@phys.uni-sofia.bg

Abstract. We propose a fast and efficient technique to create classes of highly entangled states of trapped ions, such as arbitrary Dicke states and superpositions of them, e.g. NOON states. The ions are initialized in the phonon ground state and are addressed globally with a composite pulse that is resonant with the first motional sideband. The technique is fairly robust to parameter fluctuations and operates on comparatively short time scales, as resonant interactions allow one to use the minimum laser pulse area. The number of single pulses from the composite sequence is equal to the number of ions; thus the implementation complexity grows only linearly with the size of the system. The approach does not require individual addressing of the ions in the trap and can be applied both inside and outside the Lamb–Dicke regime.

[3] Author to whom any correspondence should be addressed.

IOP Institute of Physics · DEUTSCHE PHYSIKALISCHE GESELLSCHAFT

Contents

1. Introduction

Entanglement is the most distinctive feature of quantum states involving many particles. Within the framework of quantum information science, it may be viewed as a resource for the processing of information in ways not permitted by classical logic [1]. Entanglement has various physical applications such as dense coding, quantum teleportation, quantum cryptography, quantum metrology, etc [2], which are essential for quantum communication and information processing (QIP). It is indisputable that entanglement plays a key role in QIP as quantum computers are implemented by many-body systems, generally characterized by multi-partite entangled states. Since the primary resource for quantum computation is a Hilbert-space dimension, which grows exponentially with the available physical resources [3], the benefits of a quantum over a classical computation increase with the size of the physical system. This has inspired intensive research aimed to create and study the properties of multi-partite entangled states.

A very prominent class of such states is Dicke states $|W_n^N\rangle$, originally introduced in [4]. They contain a given number of excitations n (qubits in state $|1\rangle$) shared evenly among all N qubits:

$$|W_n^N\rangle = \frac{1}{\sqrt{C_n^N}} \sum_k P_k |\underbrace{1, \ldots, 1}_{n}, \underbrace{0, \ldots, 0}_{N-n}\rangle, \tag{1}$$

where P_k denote the set of all permutations of the excitations and $C_n^N \equiv N!/[n!(N-n)!]$. Notably, Dicke states are immune against collective dephasing, which is a dominant source of decoherence in various systems, such as trapped ions [5]. Therefore, while still offering exponential dimensionality (of $C_{N/2}^N \approx 2^N/\sqrt{\pi N/2}$, example for $n = N/2$), the Dicke manifold can be used as a decoherence-free computational subspace, as in [6]. Dicke states generalize W states, which can be used for quantum communication [7]. Furthermore, Dicke states exhibit genuine multi-partite entanglement [8], which is robust against particle loss and is highly resilient versus external perturbations and measurements on single qubits [9]. Thus, Dicke states can serve as a versatile resource for the preparation of multiparticle entangled states; through projective measurements on some of the qubits one can obtain states from various entanglement

classes. Due to their robust entanglement, these states are particularly well suited for the experimental examination of multi-partite entanglement and can be used to test fundamental concepts of quantum mechanics.

Theoretical proposals exist for the generation of Dicke states in a number of physical systems, including ensembles of neutral atoms [10], trapped ions [11, 12], quantum dots [13] and using linear optics [14]. Of these, ion traps are perhaps the best suited for their unparalleled level of experimental control. We note, however, that the existing trapped-ion proposals possess one or a combination of the following drawbacks: (i) they cannot create arbitrary but only particular Dicke states, and thus do not offer a general approach; (ii) individual ion addressing is required, which poses significant experimental challenges to scalability; (iii) the number of physical interactions needed scales very fast with the system size; (iv) initialization in a particular Fock state is required; (v) Dicke states are achieved with some probability and post selection is required; and (vi) adiabatic techniques require, in general, very long interaction times. Consequently, extending the proposed techniques to larger system sizes remains a formidable challenge.

In this paper, we take a different approach and propose a simple, general and very efficient technique for the creation of a large class of highly entangled states in systems of trapped ions. These can be arbitrary Dicke states and a superposition of these, such as NOON states, which are invariant, up to a phase, under the exchange of any two ions. In addition to its generality, the proposed technique is particularly advantageous due to several features. It uses composite pulse sequences—a series of laser pulses, each with a particular area and phase. Composite pulses are a conceptually simple and very powerful control tool that enjoys large popularity in experimental physics. Although they were first developed for the needs of NMR, they were successfully applied to trapped-ion systems where many major accomplishments have been made, for example in the field of quantum information processing [15]. Their simplicity and efficacy in controlling quantum systems stem from the basic physical notion of interference. Thus, using specially designed composite pulses, our technique requires much fewer interaction steps compared to the traditional approaches, exploiting the quantum circuits of a large number of concatenated one- and two-qubit gates: the number of pulses in our approach is equal to the number of ions. Therefore, it grows only linearly with the system size, thus offering only moderate levels of experimental complexity. Another advantage of our method is that it assumes collective interaction with all ions and does not require us to manipulate exclusively individual ions or pairs of such with focused laser beams; this often presents a principal experimental challenge. The laser fields are resonant with the first motional sideband transition of the ions, which results in short interaction times, as opposed to adiabatic techniques. Our technique is also applicable outside of the Lamb–Dicke regime. This offers the possibility to overcome various detrimental effects, such as light shifts and off-resonant excitations [16], which might occur in experimental implementations.

2. The model

2.1. Hamiltonian

We consider N ions confined in a linear Paul trap, which are cooled to their vibrational ground state. Each ion has two relevant internal states $|0\rangle$ and $|1\rangle$, with respective transition frequencies ω_0. The linear ion crystal interacts uniformly with a laser pulse tuned on one of the

sidebands of the (longitudinal) center-of-mass mode, with frequency $\omega_L = \omega_0 \pm \omega_{tr}$, where ω_{tr} is the axial trap frequency. The plus sign stands for the blue sideband, while the minus sign is for the red sideband. After making the optical and vibrational rotating-wave approximations, the interaction Hamiltonian in the interaction representation for the red and blue sidebands, respectively, has the form [17]

$$\hat{H}_{I,R} = \tfrac{1}{2}\hbar g(t)\hat{a}(\eta)\hat{J}_+ + \text{H.c.,} \tag{2a}$$

$$\hat{H}_{I,B} = \tfrac{1}{2}\hbar g(t)\hat{a}^\dagger(\eta)\hat{J}_+ + \text{H.c.,} \tag{2b}$$

where $g(t) = \eta\Omega(t)\exp(-\eta^2/2)/\sqrt{N}$ is the coupling of the internal atomic states to the vibrational mode, producing pulse area $A = \int_{-\infty}^{\infty} g(t)\,\mathrm{d}t$, η is the single-ion Lamb–Dicke parameter and $\Omega(t)$ is the real-valued time-dependent Rabi frequency. Here $\hat{a}(\eta) = \sum_{n=0}^{\infty}(n+1)^{-1/2}L_n^1(\eta^2)|n\rangle\langle n+1|$ and $\hat{a}^\dagger(\eta) = [\hat{a}(\eta)]^\dagger$ are the phonon lowering and raising operators, $L_n^a(x)$ being the generalized Laguerre polynomial. $\hat{J}^\pm = \sum_{k=1}^{N} \mathrm{e}^{\pm\mathrm{i}\varphi_k}\sigma_k^\pm$, where φ_k is the phase of the laser field interacting with the kth ion, and $\sigma_k^+ = |1_k\rangle\langle 0_k|$ and $\sigma_k^- = |0_k\rangle\langle 1_k|$ are the raising and lowering operators for the internal states of the kth ion. In the Lamb–Dicke limit the operators $\hat{a}^\dagger(\eta)$ and $\hat{a}(\eta)$ become the ordinary creation and annihilation operators of the center-of-mass phonons.

We now perform the transformation $|1_k\rangle \rightarrow |\widetilde{1}_k\rangle\mathrm{e}^{-\mathrm{i}\varphi_k}$, thereby incorporating the laser phase into the atomic states. As a result, the Hamiltonian is recast in terms of the usual pseudospin operators $\hat{J}^\pm = \sum_{k=1}^{N} \widetilde{\sigma}_k^\pm$. The energy pattern splits into manifolds corresponding to n atomic and ν motional excitations (figure 1(a)). For red-sideband interaction, we have $n + \nu = m_R$, i.e. the total number of quanta m_R is conserved, while for blue sideband we have $n - \nu = m_B$, i.e. the difference of the quanta is conserved. To create symmetric entangled states, a suitable choice is $m_R = N$ and $m_B = 0$. Although our method is equally applicable for both, in what follows we will assume blue-sideband interaction.

Figure 1(a) depicts all states which are accessible if one starts from the ground state $|000\rangle|0\rangle$. The example given is for a chain of $N = 3$ ions. The ions interact with a blue-sideband laser field, $\omega_L = \omega_0 + \omega_{tr}$, which couples equally each ion's internal state to the collective motional center-of-mass mode: $|0_k\rangle|\nu\rangle \leftrightarrow |1_k\rangle|\nu+1\rangle$. The system is described by the anti-Jaynes–Cummings Hamiltonian (2b). To this end, we adopt the wavefunction notation $|\psi\rangle|\nu\rangle$, where $|\psi\rangle = |q_1 q_2, \ldots, q_{n+1}\rangle$ is the collective internal state of the ion qubits, with $q_k = 0$ or 1, and $|\nu\rangle$ is the vibrational Fock state of ν phonons.

2.2. Hilbert space factorization

In order to study the dynamics of our system, it is convenient to introduce a new basis which consists of the set of eigenvectors of the two commuting pseudospin operators $\hat{J}^2$ and $\hat{J}_z$, where $\hat{J}^2 = \tfrac{1}{2}(\hat{J}_+\hat{J}_- + \hat{J}_-\hat{J}_+) + \hat{J}_z^2$. This approach was also used in [6]. Each state is assigned two quantum numbers, j and m_j, respectively. Since $\hat{J}^2$ commutes with the Hamiltonian, the Hilbert space factorizes into a set of decoupled chains with different values of j; the Hamiltonian preserves j. The meaning of this becomes more transparent if we note that $\hat{J}^2 = \sum_{k,l=1}^{N} \tfrac{1}{2}S_{kl} - \tfrac{1}{4}(-1)^{\delta_{kl}}\mathbf{1}$, with $S_{kl} = \sigma_k^+\sigma_l^- + \sigma_k^-\sigma_l^+ + \tfrac{1}{2}\sigma_{k,z}\sigma_{l,z} + \tfrac{1}{2}(-1)^{\delta_{kl}}\mathbf{1}$ denoting the action of the swapping operator, which exchanges ions k and l. Therefore, each j stands for a particular symmetry with respect to exchanging ions. Since our class of target states is invariant under the action of each S_{kl}, it comprises the eigenstates of S_{kl} with unit eigenvalue.
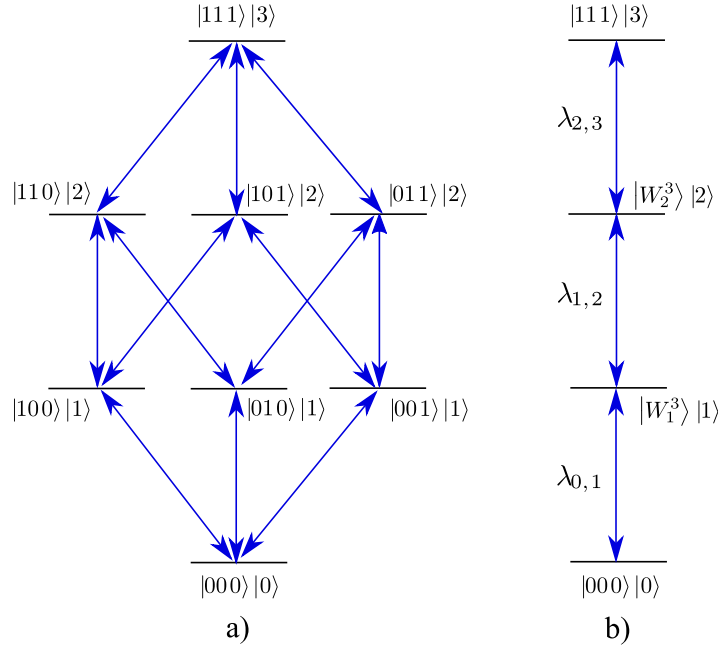
Figure 1. (a) Linkage pattern of the collective states of $N = 3$ trapped ions equally coupled to their common center-of-mass mode by a uniform laser field. The difference between the number of ionic excitations n and the number of vibrational phonons $\nu = n$ is conserved. The laser beam is tuned to the blue-sideband resonance, $\omega_L = \omega_0 + \omega_{tr}$. (b) Chains comprising symmetric Dicke states $|W_n^N\rangle|\nu\rangle$ for $N = 3$. These constitute the whole set of states that can be accessed by a uniform laser driving starting from the state $|00\cdots0\rangle|0\rangle$. The states are coupled resonantly on the first blue sideband with $\lambda_{\nu-1,\nu}(t)$ being the coupling strengths.

Thus, the eigenvalue of $\hat{J}^2$ is $(1 + N/2)N/2$. Hence, the chain containing our states is assigned $j = N/2$, and by analogy with the traditional angular momentum operators, the number of states is equal to $2j + 1 = N + 1$. These are all Dicke states $|W_n^N\rangle|\nu\rangle$, with n being the number of atomic excitations: $n = 0, \ldots, N$. Hence, all states we are interested in are contained in a single chain, and are coupled by the Hamiltonian (2b) in the order given (figure 1(b)). As long as the interaction with the ions is distributed uniformly, the dynamics is enclosed in this chain as it gets decoupled from the rest of the Hilbert space. The states differ by energy, which is measured by the operator $\hat{J}_z$. Its eigenvalues m_j vary from $-j$ to j and define the number of excited ions, $n = j + m_j = N/2 + m_j$.

For the following analysis, it will be necessary to go further and calculate the coupling coefficients in the new basis. The coupling between the neighbors $|j, m_j\rangle$ and $|j, m_j - 1\rangle$ follows immediately from the matrix elements of the operators $\hat{a}^\dagger(\eta)$, $\hat{a}(\eta)$ and $\hat{J}_\pm$:

$$\lambda_{\nu-1,\nu}(t) = g(t)L_{\nu-1}^1(\eta^2)\sqrt{N - \nu + 1}. \tag{3}$$

In the following, for conciseness we will consider only operation inside the Lamb–Dicke regime, which requires $\eta \ll 1$.

3. Implementation

Our method begins with the initialization of the string of N ions in the collective internal and vibrational ground state $|\psi\rangle|\nu\rangle = |00\cdots0\rangle|0\rangle$.[4] For ease of notation, the indices in $|\psi\rangle$ denoting states will be omitted hereafter.

3.1. Creation of Dicke states

The N-ion Dicke states $|W_n^N\rangle|\nu\rangle$ are constructed in the following way. A series of N pulses is applied globally on all ions, each pulse having a particular area A_k and phase ϕ_k. The pulses are resonant with the first blue sideband relative to the center-of-mass (COM) mode, i.e. the carrier frequencies are $\omega_L = \omega_0 + \omega_{tr}$. Thereby the state $|00\cdots0\rangle|0\rangle$ is coupled to all states $|W_n^N\rangle|n\rangle$, shown in figure 1(b). If other modes are used, one would connect states of another symmetry. Because resonant interactions are employed, the dynamics is defined only by the pulse areas A_k and does not depend on the temporal pulse shape.

To study the effect of this interaction we derive the propagator $U(A_k, \phi_k)$ describing the dynamics of the chain of Dicke states (figure 1(b)), subject to a laser pulse of area A_k and phase ϕ_k. This is done by exact diagonalization and exponentiation of the Hamiltonian, $U(A_k, \phi_k) = \exp(-\frac{i}{\hbar}\int \hat{H}_{I,B}\, dt)$, with the coupling in $\hat{H}_{I,B}$ being phased, $g(t) \rightarrow g(t)e^{i\phi_k}$. The total sequence of N pulses, having area $A_{tot} = \sum_{k=1}^{N} A_k$, is represented by the propagator

$$U_{tot} = U(A_N, \phi_N)U(A_{N-1}, \phi_{N-1})\cdots U(A_1, \phi_1). \tag{4}$$

We fix $\phi_1 = 0$, which defines our phase reference. Hence, the total propagator U_{tot} is defined by N pulse areas and $N-1$ phases, a total of $2N-1$ variables, which can be varied as free parameters.

Dicke states, or various superpositions of these, are obtained for specific sets of parameters, which are determined numerically through maximizing the fidelity with the target state $|t\rangle$, seeking unity. The fidelity is defined as

$$\mathcal{F}(A_k, \phi_k, t) = |\langle t|U_{tot}|00\cdots0\rangle|0\rangle|^2 \tag{5}$$

and is a function of all areas A_k and phases ϕ_k. The numerical optimization procedure runs over the $2N-1$ dimensional space of A_k and ϕ_k and follows Newton's gradient-based method. Because this is a local optimization algorithm, we iteratively pick the initial parameter values using the Monte-Carlo scheme. Out of the many solutions obtained, we select the one having the minimal total pulse area A_{tot}.

The numerical optimization is computationally not difficult even beyond $N = 15$ ions, even though the dimension of the Hilbert space scales exponentially with N. The reason is that the system resides only in the chain of symmetric states of dimension $N + 1$, shown in figure 1(b).

In table 1 we provide examples of pulse sequences which yield Dicke states $|W_n^N\rangle$ for different numbers of ions N. We choose $n = \lfloor N/2 \rfloor$, $\lfloor x \rfloor$ being the integer part of x. In a real experiment one may not be able to set the control parameters exactly as prescribed by table 1. The fluctuations around the optimal values would result in a decrease of the fidelity. We have investigated this scenario and the result is shown in figure 2 (top), which illustrates the final fidelity for different Dicke states versus the standard deviations of the control parameters A_k

---

[4] This does not necessarily impose the Lamb–Dicke (LD) regime, which is accessed when both the phonon number and the LD parameter are very small.

Table 1. Exemplary areas A_k and phases ϕ_k (in units of π) for composite pulse sequences, which produce N-ion Dicke states $|W_n^N\rangle$. We choose $n = \lfloor N/2 \rfloor$, where $\lfloor x \rfloor$ is the integer part of x. The composite sequences are described by the propagator (4) and comprise N phased pulses, tuned on the first blue sideband. It is noteworthy that for increasing values of N the total pulse area A_{tot} is less than $(N/2)\pi$ (we have checked that this property holds also for $N > 10$).

		Dicke states, $|W_n^N\rangle$
N	A_{tot}	$(A_1, \phi_1;\ A_2, \phi_2;\ \dots;\ A_N, \phi_N)$
3	2.53	(0.369, 0; 0.484, 2.39; 1.682, 2.976)
4	2.28	(0.805, 0; 0.495, 1.728; 0.793, 0.566; 0.191, 0.079)
5	2.11	(0.795, 0; 0.278, 0.403; 0.480, 0.075; 0.223, 0.309; 0.333, 0.915)
6	2.12	(0.562, 0; 0.315, 1.478; 0.343, 0.854; 0.277, 0.417; 0.126, 0.091; 0.501, 1.423)
7	2.15	(0.107, 0; 0.584, 1.694, 0.562, 1.566, 0.497, 1.313, 0.039, 1.956, 0.158, 1.301, 0.206, 1.847)
8	2.46	(0.539, 0; 0.216, 0.389; 0.459, 0.098; 0.251, 1.560; 0.464, 0.816; 0.25, 0.388; 0.25, 2.078; 0.03, 1.607)
9	3.35	(0.51, 0; 0.234, 0.83; 0.9, 0.304; 0.19, 2.025; 0.352, 0.164; 0.379, 0.556; 0.358, 0.097; 0.199, 0.239; 0.231, 0.471)
10	3.89	(0.621, 0; 0.367, 1.147; 0.097, 0.994; 0.616, 1.709; 0.113, 0.263; 0.203, 0.661; 0.579, 0.328; 0.223, 0.831; 0.775, 0.909; 0.292, 0.462)

and ϕ_k. It is noteworthy that the calculated fidelity stays well above 95% for deviations of the order of 1%, which are typical for the present state-of-the-art technology [18].
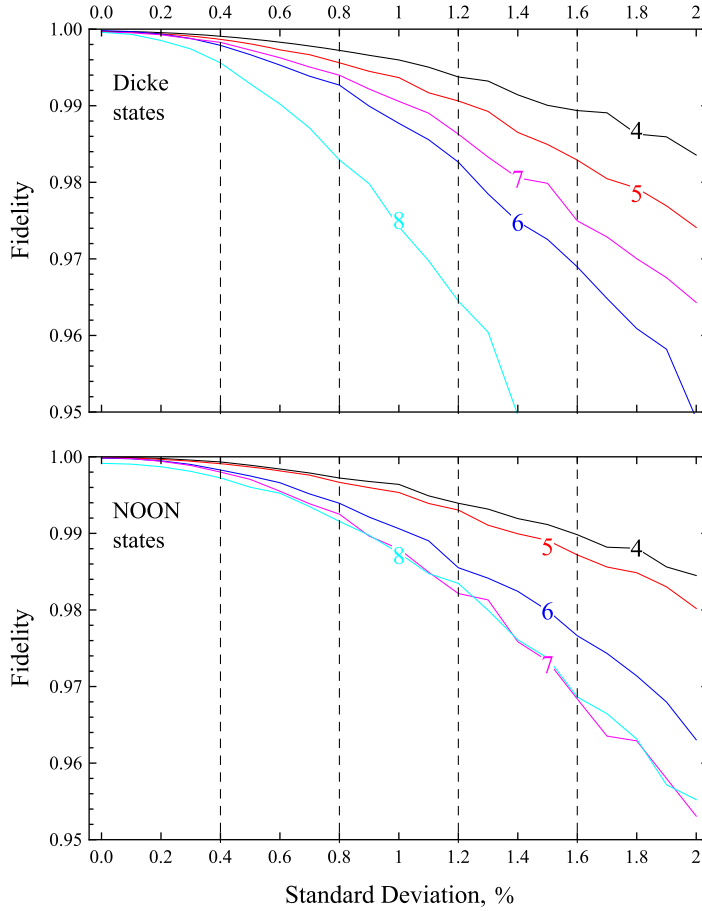
3.2. Creation of NOON states

We can also create arbitrary superpositions of the states contained in the chain of accessible states, shown in figure 1(b). Of particular interest is the possibility to generate NOON states $|N^N\rangle$, which are another very important class of highly nonclassical entangled states. They can be defined as an equal-probability superposition of two Dicke states $|W_n^N\rangle$, whereby the excitation is contained either in the internal state or in the motional state of the ions: $|N^N\rangle = |W_N^N\rangle|0\rangle + |W_0^N\rangle|N\rangle \equiv |11\cdots1\rangle|0\rangle + |00\cdots0\rangle|N\rangle$ (for simplicity, normalization constants are omitted throughout). The ions are maximally correlated, as measuring the state of one ion determines the state of all N ions.

Various applications of NOON states of both fundamental and practical interest have been suggested, for example entanglement enhanced metrology and sub-wavelength lithography [19, 20]. Different schemes for the creation of NOON states in trapped-ion systems have been proposed theoretically [19, 21] and realized experimentally [22]. However, they are subject to requirements for individual ion addressing, a limited number of ions or long interaction times where adiabaticity is employed.

Unlike the previous proposals, our method allows us, by using global addressing, to create arbitrary NOON states. As the interaction is resonant, the states are created on short time scales. We perform the same manipulation as for the creation of Dicke states—a sequence of laser

Figure 2. Fidelity for the creation of various Dicke (top) and NOON states (bottom) versus the standard deviation in the control parameters A_k and ϕ_k, with $k = 1, \ldots, N$. The parameters are listed in tables 1 and 2, respectively, and the numbers denote the number of ions N.

pulses is applied, each addressing globally the chain of ions and having a particular area A_k and a relative phase ϕ_k. The pulses are resonant with the first blue-sideband transition. For particular pulse sequences one obtains the coherent superposition $|W_0^N\rangle|0\rangle + |W_N^N\rangle|N\rangle$. If we logically interchange $|0\rangle$ and $|1\rangle$, $|0\rangle \leftrightarrow |1\rangle$, this state corresponds to the NOON state $|N^N\rangle$.

In table 2, we provide examples of pulse sequences, which yield NOON states $|N^N\rangle$ for different numbers of ions N. Figure 2 (bottom) illustrates the final fidelity of various NOON states versus the standard deviations of the control parameters A_k and ϕ_k. As for the Dicke states, the calculated fidelity stays well above 95% for deviations of the order of 1%.

3.3. Rate of creation of the target states

As already mentioned, the proposed technique operates on comparatively short time scales. An estimate of the duration of the composite pulse sequences needed to create our symmetric entangled states is given by $T_{tot} = A_{tot}/g$. In order to suppress the excitation of the extraneous phonon modes (other than the center-of-mass mode), we limit the coupling strength from above

Table 2. Exemplary areas A_k and phases ϕ_k (in units of π) for composite pulse sequences, which produce N-ion NOON states $|N^N\rangle$. The sequences are described by the propagator (4) and comprise N phased pulses, tuned on the first blue sideband. It is noteworthy that for increasing values of N the total pulse area A_{tot} is below $(N/3)\pi$ (we have checked that this property holds also for $N > 10$).

		NOON states, $|N^N\rangle$
N	A_{tot}	$(A_1, \phi_1; A_2, \phi_2; \ldots; A_N, \phi_N)$
3	1.60	(0.696, 0; 0.640, 1.511; 0.259, 1.962)
4	1.63	(0.402, 0; 0.291, 0.151; 0.667, 1.819; 0.271, 1.465)
5	1.88	(0.494, 0; 0.249, 0.652; 0.651, 1.271; 0.313, 0.806; 0.175,1.175)
6	1.83	(0.284, 0; 0.235, 0.219; 0.099, 0.701; 0.673, 1.178; 0.403, 0.665; 0.136, 1.022)
7	2.06	(0.278, 0; 0.300, 0.266; 0.338, 0.034; 0.541, 1.895; 0.277, 2.138; 0.137, 0.662; 0.187, 0.070)
8	2.33	(0.259, 0; 0.923, 0.209; 0.346, 0.408; 0.428, 1.572; 0.003, 1.705; 0.204, 1.216; 0.003, 2.11; 0.162, 1.543)
9	2.46	(0.395, 0; 0.146, 2.556; 0.186, 1.336; 0.237, 1.854; 0.680, 0.740; 0.452, 1.660; 0.169, 0.862; 0.007, 0.222; 0.186, 1.555)
10	2.93	(0.476, 0; 0.239, 1.247; 0.289, 1.380; 0.256, 0.305; 0.228, 2.021; 0.415, 0.220; 0.388, 0.749; 0.059, 1.718; 0.529, 1.823; 0.047, 0.861)

to $g = \omega_{\text{tr}}/10$ [23]. If we assume a typical trap frequency of $\omega_{\text{tr}} = 4$ MHz, as in [24], and $A_{\text{tot}} \approx 2\pi$ as obtained in the above examples for the creation of $|W_3^6\rangle$ and $|N^6\rangle$, we obtain $T_{\text{tot}} \approx 15\,\mu$s. For comparison, in [11] the Dicke state $|W_2^6\rangle$ is created adiabatically in $400\,\mu$s.

Importantly, as can be seen from tables 1 and 2, for increasing the number of ions N the total pulse area A_{tot} stays below $(N/2)\pi$ for Dicke states and below $(N/3)\pi$ for NOON states. Therefore, the duration T_{tot} increases only linearly with N and is asymptotically limited by $(N/2)T_\pi$ and $(N/3)T_\pi$, respectively, $T_\pi \approx 8\,\mu$s being the duration of a π pulse.

4. Conclusions

We have proposed a simple and efficient technique for the creation of arbitrary collective states of trapped ions, which are symmetric under exchange of any two ions. These can be Dicke states and superpositions of these, such as NOON states. The method uses dedicated composite sequences of phased resonant pulses tuned on the first red or blue motional sideband of the center-of-mass mode. The composite sequences comprise N pulses, N being the number of ions; thus the implementation complexity and duration grow only linearly. This is in contrast to other proposals which require a rapidly increasing number of elementary gates, demanding exclusive interaction with single ions or pairs of ions. As opposed to previous proposals, the ions are addressed globally; thus individual ion access is unnecessary. Due to the resonant type of interaction and because the required by our method total pulse area is as low as $(N/2)\pi$, the states are created on a comparatively short time scale. The method is applicable also outside of the Lamb–Dicke regime.

IOP Institute of Physics **Φ** DEUTSCHE PHYSIKALISCHE GESELLSCHAFT

Acknowledgments

References

[1] Nielsen M A and Chuang I L 2000 *Quantum Computation and Quantum Information* (Cambridge: Cambridge University Press)

[2] Bennett C H and Wiesner S J 1992 *Phys. Rev. Lett.* **69** 2881–4
Mattle K, Weinfurter H, Kwiat P G and Zeilinger A 1996 *Phys. Rev. Lett.* **76** 4656
Bennett C H, Brassard G, Crepeau C, Jozsa R, Peres A and Wootters W K 1993 *Phys. Rev. Lett.* **70** 1895
Boschi D, Branca S, De Martini F, Hardy L and Popescu S 1998 *Phys. Rev. Lett.* **80** 1121
Bennett C H and Brassard G 1984 *Proc. IEEE Int. Conf. on Computers, Systems and Signal Processing (Bangalore)* pp 175–9

[3] Blume-Kohout R, Caves C M and Deutsch I H 2002 *Found. Phys.* **32**

[4] Dicke R H 1954 *Phys. Rev.* **93** 99

[5] Lidar D A and Whaley K B 2003 *Lect. Notes Phys.* **622** 83

[6] Ivanov S S, Ivanov P A, Linington I E and Vitanov N V 2010 *Phys. Rev.* A **81** 042328
Ivanov S S, Ivanov P A and Vitanov N V 2008 *Phys. Rev.* A **78** 030301(R)
Linington I E, Ivanov P A and Vitanov N V 2009 *Phys. Rev.* A **79** 012322

[7] Joo J, Park Y-J, Lee J, Jang J and Kim I 2005 *J. Korean Phys. Soc.* **46** 763–8
Joo J, Lee J, Jang J and Park Y-J 2002 arXiv:quant-ph/0204003v2
Buhrman H, van Dam W, Høyer P and Tapp A 1999 *Phys. Rev.* A **60** 2737–41

[8] Tóth G 2007 *J. Opt. Soc. Am.* B **24** 275
Usha Devi A R, Prabhu R and Rajagopal A K 2007 *Phys. Rev. Lett.* **98** 060501

[9] Stockton J K, Geremia J M, Doherty A C and Mabuchi H 2003 *Phys. Rev.* A **67** 022112
Bourennane M, Eibl M, Gaertner S, Kiesel N, Kurtsiefer C and Weinfurter H 2006 *Phys. Rev. Lett.* **96** 100502
Dür W 2001 *Phys. Rev.* A **63** 020303

[10] Stockton J K, van Handel R and Mabuchi H 2004 *Phys. Rev.* A **70** 022106
Mandilara A, Akulin V M, Kolar M and Kurizki G 2007 *Phys. Rev.* A **75** 022327
Thiel C, von Zanthier J, Bastin T, Solano E and Agarwal G S 2007 *Phys. Rev. Lett.* **99** 193602

[11] Linington I E and Vitanov N V 2008 *Phys. Rev.* A **77** 010302

[12] Retzker A, Solano E and Reznik B 2007 *Phys. Rev.* A **75** 022312
López C E, Retamal J C and Solano E 2007 *Phys. Rev.* A **76** 033413
Häffner H *et al* 2005 *Nature* **438** 643
Hume D B, Chou C W, Rosenband T and Wineland D J 2009 *Phys. Rev.* A **80** 052302

[13] Zou X B, Pahlke K and Mathis W 2003 *Phys. Rev.* A **68** 034306

[14] Kiesel N, Schmid C, Tóth G, Solano E and Weinfurter H 2007 *Phys. Rev. Lett.* **98** 063604
Thiel C, von Zanthier J, Bastin T, Solano E and Agarwal G S 2007 *Phys. Rev. Lett.* **99** 193602

[15] Monz T *et al* 2009 *Phys. Rev. Lett.* **102** 040501
Schmidt-Kaler F *et al* 2003 *Nature* **422** 408
Gulde S *et al* 2003 *Nature* **421** 48
Schmidt-Kaler F *et al* 2003 *Appl. Phys.* B **77** 789
Childs A M and Chuang I L 2000 *Phys. Rev.* A **63** 012306

[16] Steane A, Roos Ch F, Stevens D, Mundt A, Leibfried D, Schmidt-Kaler F and Blatt R 2000 *Phys. Rev.* A **62** 042305

[17] Leibfried D, Blatt R, Monroe C and Wineland D 2003 *Rev. Mod. Phys* **75** 281

IOP Institute of Physics Φ DEUTSCHE PHYSIKALISCHE GESELLSCHAFT

[18] Häffner H, Roos C F and Blatt R 2008 *Phys. Rep.* **469** 155–203

[19] Bollinger J J, Itano W M, Wineland D J and Heinzen D J 1996 *Phys. Rev.* A **54** R4649

[20] Edamatsu K, Shimizu R and Itoh T 2002 *Phys. Rev. Lett.* **89** 213601
  Boto A N *et al* 2000 *Phys. Rev. Lett.* **85** 2733
  D'Angelo M, Chekhova M V and Shih Y 2001 *Phys. Rev. Lett.* **87** 013602
  Huelga S F *et al* 1997 *Phys. Rev. Lett.* **79** 3865

[21] Boixo S, Datta A, Davis M J, Shaji A, Tacla A B and Caves C M 2009 *Phys. Rev.* A **80** 032103
  Hu Y M, Feng M and Lee C 2011 arXiv:1110.1429v2

[22] Leibfried D, Barrett M D, Schaetz T, Britton J, Chiaverini J, Itano W M, Jost J D, Langer C and Wineland D J 2004 *Science* **304** 1476
  Sackett C A *et al* 2000 *Nature* **404** 256

[23] James D F V 1998 *Appl. Phys.* **66** 181

[24] Schmidt-Kaler F, Gulde S, Riebe M, Deuschle T, Kreuter A, Lancaster G, Becher C, Eschner J, Häffner H and Blatt R 2003 *J. Phys. B: At. Mol. Opt. Phys.* **36** 623